Established 1833

Awarded:

Mainz 1842 · Berlin 1844 · London 1854 · Paris 1855 · London 1862
Paris 1867 · Sidney 1879 · Bologna 1881 · Antwerpen 1885
Chicago 1893 · Brüssel 1897

DR F. KRANTZ
RHENISH MINERAL-OFFICE
MANUFACTURER OF APPARATUS FOR THE TEACHING
MINERALOGY AND GEOLOGY
IN
BONN O. RH., GERMANY

Catalogue Nr 15

Penfield-Collection of 225 Crystal-Models

in peartree-wood for illustrating Chapter V of the

BRUSH-PENFIELD: Determinative Mineralogy and Blowpipe Analysis

Catalogue Nr. 1a: Minerals
" " 1b: Crystal-Models
" " 2a: Geology
" " 2b: Palaeontology
" " 3: Gypsum models (ill.)
" " 4*): Rocks and Thin sections
free by post to all parts of the world.

*) with Supplement 1–3

CONDITIONS OF SALE

1. Our **prices** are fixed without liability and payable at Bonn at three months with $1^1/_2$ % discount on payments made within thirty days. After the expiration of three months, we will draw a draft or postal order for the amounts not then liquidated. Persons not known to us must pay in advance but are allowed a discount of $1^1/_2$ % for so doing.

2. **Public institutions** will be given special terms of payment according to their resp. funds.

3. Consignees may return single specimens out of a lot of minerals or fossils and which do not suit them within thirty days after their receipt and exchange them for other specimens or receive an allowance therefore, but the return carriage must be at their own expense.

4. **Trial consignments** will be sent to responsible persons with the privilege of examination; those not retained must be returned, well packed, and in good order, and at the expense and risk of the consignee, within two weeks after receipt.

5. **Crystal models**, rocks, thin sections of rocks, plates of minerals, plastermodels, geological models and all apparatus, instruments, tools and utensils will be sent only on a positive order.

6. Orders for wooden-, glass- or paste-board-models of crystals and for geotectonic models not found in the catalogue, but accompanied by accurate drawings, will be promptly executed.

7. Specimens will be **packed** with great care, by experienced workman and in the best manner, and the material used in packing will be charged for at cost.

ESTABLISHED 1833

Awarded: Mainz 1842 · Berlin 1844 · London 1854
Paris 1855 · London 1862 · Paris 1867 · Sidney 1879
Bologna 1881 · Antwerpen 1885 · Chicago 1893
Brüssel 1897

D^R^ F. KRANTZ

RHENISH MINERAL-OFFICE

MANUFACTURER OF APPARATUS FOR THE TEACHING
MINERALOGY AND GEOLOGY
IN

BONN O. RH., GERMANY

Catalogue Nr 15

Penfield-Collection of 225 Crystal-Models

in peartree-wood for illustrating Chapter V of the

BRUSH-PENFIELD: Determinative Mineralogy and Blowpipe Analysis

Catalogue Nr. 1a: Minerals
" " 1b: Crystal-Models
" " 2a: Geology
" " 2b: Palaeontology
" " 3: Gypsum models (ill.)
" " 4*): Rocks and Thin sections (with supplements 1—3)
free by post to all parts of the world.

PRICE-LIST

The Penfield-collection of 225 crystal-models in peartree-wood average size of 5 cm = *M* 230.—
„ „ „ 10 „ = „ 615.—

Single numbers from this collection are sold at the following prices (If at least 3 or 6 pieces of the same number be ordered, a reduction of 5 % and 10 % resp. will be allowed):

Nr.	5 cm *M*	10 cm *M*	Nr.	5 cm *M*	10 cm *M*	Nr.	5 cm *M*	10 cm *M*	Nr.	5 cm *M*	10 cm *M*
1	1.—	2.—	36	1.35	3.—	71	1.20	3.—	106	—.85	2.50
2	1.—	2.—	37	1 35	3.35	72	1.35	3.—	107	—.85	2.50
3	1.20	2.50	38	1.65	4.20	73	1.35	3.35	108	1.20	3.—
4	1.35	3.—	39	1.—	3.—	74	1.20	3.35	109	1.20	3.—
5	1.35	3.—	40	1.—	3.—	75	1.20	3.35	110	1.—	2.50
6	1.35	3.—	41	1.35	3 —	76	1.35	3.35	111	—.85	3.—
7	1.35	3.—	42	1.35	3.—	77	—.85	2.00	112	1.20	3 —
8	1.35	3.—	43	1.35	3.—	78	1.—	2.50	113	2.50	5.85
9	1.35	3.—	44	1.35	3.—	79	—.85	2.—	114	1.20	3.—
10	1.35	3.35	45	1.—	2.50	80	1.—	2.50	115	2.50	5.85
11	1.35	3.35	46	1.—	2.50	81	2.50	5.85	116	1.35	3.35
12	2.65	5.85	47	1.—	2.50	82	1.65	4.20	117	1.35	3.35
13	2.50	5.—	48	1.—	2.50	83	1.20	3.—	118	1.35	3.35
14	1.35	3.—	49	1.35	3.—	84	1.20	3.—	119	1.20	3.—
15	1.35	3 35	50	—.85	2.—	85	1.35	3.35	120	1.35	3.35
16	1.35	3.35	51	—.85	2.—	86	—.85	2.50	121	1.35	3.—
17	1.65	3 35	52	1.—	2.50	87	—.85	2.50	122	1.—	2 50
18	1.35	3.—	53	1.—	2.50	88	1.—	3.—	123	1.—	3.—
19	1.35	3.35	54	1.—	2.50	89	1.20	3.—	124	1.35	3.35
20	1 35	3.—	55	1.20	3.—	90	1.20	3.—	125	1.65	4.20
21	1.35	3.35	56	1.20	3.—	91	1.20	3.—	126	1.35	3.35
22	2.—	4.20	57	1.35	3.35	92	1.35	4.20	127	1.35	3.—
23	2.—	5.—	58	1.—	2.50	93	—.85	1.65	128	1.35	3.—
24	2.—	5.—	59	1.20	3.—	94	1.35	3.—	129	1.35	3.35
25	1.20	3.—	60	1.20	3.—	95	1.20	2.—	130	1.35	3.—
26	1.35	3.35	61	1.20	3.—	96	2.—	5.—	131	1.35	3.35
27	1.35	3.—	62	1.20	3.—	97	1.20	3.—	132	1.20	3.—
28	1.35	3.—	63	2.50	5.85	98	1.20	3.—	133	1.35	3.35
29	1.35	3.35	64	2.50	5.85	99	1.20	3.—	134	1.20	3.—
30	1.35	3.35	65	1.35	3.—	100	1.35	3.35	135	1.35	3.35
31	1.65	3.35	66	1.35	3.—	101	1.35	3.35	136	1.20	3.35
32	1.65	4.20	67	1.20	2.55	102	1.—	2.50	137	1.20	3.—
33	5.85	10.—	68	1.20	3.—	103	1.—	2.50	138	1.—	2.50
34	—.85	2.—	69	1.20	3.—	104	1.35	3.—	139	1.35	3.35
35	—.85	2.—	70	1.20	3.—	105	—.85	2.50	140	1.35	3.35

Nr.	5 cm M	10 cm M	Nr.	5 cm M	10 cm M	Nr.	5 cm M	10 cm M	Nr.	5 cm M	10 cm M
141	1.35	3.35	163	1.20	3.—	185	1.20	2.50	207	1.35	3.35
142	1.20	3.35	164	1.20	3.—	186	1.20	2.50	208	1.35	3.35
143	1.20	3 35	165	1.35	3.35	187	1.—	2.50	209	1.35	3.35
144	1.20	3.35	166	1 35	3 35	188	1.—	2.50	210	1.35	3.35
145	1.65	3.35	167	1.35	3.—	189	1.—	2.50	211	1.35	3.35
146	1.65	3 35	168	1.35	3.—	190	1.20	3.—	212	1.35	3.35
147	1.—	2.50	169	1.35	3.—	191	1.20	3.—	213	1.20	3.—
148	—.85	2.—	170	1.35	3.—	192	1.35	3.—	214	1.—	2.50
149	1.—	2.50	171	1.35	3.35	193	1.35	3.—	215	1.—	2.50
150	1.—	2.50	172	1.35	3.—	194	2.50	5.—	216	1.—	2.50
151	—.85	2.—	173	1.35	3.35	195	1.35	3.—	217	1.—	2.50
152	—.85	2.—	174	1.—	2.—	196	1.35	3.—	218	1.35	3.35
153	1.—	2.50	175	1.20	2.50	197	1.35	3.35	219	1.35	3.35
154	1.20	2.50	176	3.—	5.85	198	2.50	5.85	220	1.35	3.35
155	1.20	3.—	177	3.—	5.85	199	1.35	3.—	221	2 50	5.—
156	1 20	3.—	178	1.35	3.35	200	1.35	3.35	222	3.35	6.65
157	1.20	3.—	179	1.20	3.—	201	1.35	3.35	223	1.20	2.50
158	1.20	3.—	180	2.—	5.—	202	1.35	3.35	224	1.35	3.35
159	1 20	3.—	181	2.50	5.85	203	1.35	3.35	225	1.35	3.35
160	1.35	3.35	182	3.35	6.65	204	1.35	3.35			
161	1.20	3.—	183	1.20	3.—	205	1.20	3.—			
162	1.20	3.35	184	1.35	3.—	206	1.35	3.35			

In ordering single models the mentioning of the number will suffice.

All orders will promptly be attended.

If desired this collection will be sent post free and packed in best manner for shipment

at £ 11—10—0— resp. „ £ 31— 5—0— } as far as London

at $ 57.50 resp. „ $ 152.— } as far as New York

but in this case the remittance must be sent with the order.

In addition to this collection of 225 models we offer the new

Penfield Contact-Goniometer and Arm Protractor

which will be found most useful for the study of the models. For detailed description see pages 11—14 at the end of this catalogue.

DR F. KRANTZ
RHENISH MINERAL-OFFICE

Collection of 225 Crystal-Models

for illustrating Chapter V of the

BRUSH-PENFIELD:

Determinative Mineralogy and Blowpipe Analysis.

Chapter V of the text-book referred to was prepared by the writer for the purpose of presenting the difficult subject of crystallography in a manner as elementary as possible, yet with due regard to the changes which have been introduced in recent years in the classification of crystals. Professor Miers of Oxford in a review of the Text-Book in the Mineralogical Magazine, Vol. 12, page 127, has made the following statement concerning Chapter V: „This chapter is the simplest and most intelligible summary of the principles of Crystallography that has yet been given to the elementary student, and is a very noteworthy feature of the book.“ Practically all of the figures given in the book are reproduced in wood. Of the 32 possible classes of crystals 18 are represented in the collection, and special care has been taken to illustrate by numerous examples those groups which are most important from a mineralogical standpoint. Groups which are not represented in the collection are either of rare occurrence among mineral substances, or else unknown.

A feature of the collection is that, with only a few exceptions, the models represent prominent types or habits of common minerals; hence those studying the models will be able to compare them with actual crystals of minerals which may be found in almost any collection. The models, mereover, illustrate a very important feature of crystals, namely, that the forms which are prominent and determine the crystal habit are, with few exceptions, those to which simple indices may be assigned. On the 225 models 669 independent forms are represented, as follows:

Indices 100 or variations	(cube, pinacoids)	29%
„ 110 „ „	(dodecahedron, prisms, domes)	25%
„ 111 „ „	(octahedron, pyramids)	22%

As the collection may be regarded as fairly representive, the foregoing summary indicates that fully 75 per cent of the forms which the elementary student will probably encounter will have no other figures in their symbols than unity and zero. In making the foregoing summary it should be stated that, in the hexagonal and rhombohedral divisions, prisms and pyramids of the first order and second order, respectively, were regarded as equivalent to forms of the corresponding orders in the tetragonal system.

For each of the systems, with the exception of the isometric, a series of models of the simple forms has been made having equal axial lengths. These models, if properly orientated, will help the beginner to understand certain relations and variations exhibited by different forms which are not easily comprehended by studying the figures accompanying a text, as, for example, the relations of the prisms in the tetragonal system, and of the prisms and domes in the orthorhombic system.

The models are constructed with surprising accuracy, for which the Rheinisches Mineralien-Contor of Dr. Krantz in Bonn has long held a reputation. It is certain that those who are studying crystallography will find it a great advantage to have at hand not only models which correspond to a standart text, but, also, types which have been carefully selected as representatives of the important classes of crystals in the mineral kingdom.

New Haven, Conn., Feb. 1, 1901.

Samuel L. Penfield,
Yale University.

Isometric System.

Models 1—44.

Normal Group of the Isometric System.

Models No. 1—24.

No. 1, Fig. 95. — Cube *a* (100). — Galena, fluorite, halite.
„ 2, Fig. 96. — Octahedron *o* (111). — Galena, magnetite, fluorite.
„ 3, Fig. 97. — Dodecahedron *d* (110). — Garnet, magnetite.
„ 4 to 11. — Illustrate combinations of the cube *a* (100), octahedron *o* (111), and dodecahedron *d* (110).
„ 4, Fig. 98. — Cube *a* and octahedron *o*. — Galena, fluorite, sylvite.
„ 5, Fig. 99. — Cube *a* and octahedron *o*, sometimes called cubo-octahedron. — Galena, fluorite.
„ 6, Fig. 100. — Octahedron *o* and cube *a*. — Galena, fluorite.
„ 7, Fig. 101. — Cube *a* and dodecahedron *d*. — Fluorite.
„ 8, Fig. 102. — Octahedron *o* and dodecahedron *d*. — Magnetite, galena.
„ 9, Fig. 103. — Dodecahedron *d* and octahedron *o*. — Magnetite.
„ 10. — Dodecahedron *d*, cube *a*, and octahedron *o*. — Fluorite.
„ 11, Fig. 104. — Cube *a*, dodecahedron *d*, and octahedron *o*. — Fluorite, galena.
„ 12, Fig. 83. — Penetration cubes in twin position. — Fluorite. An octahedral face, $11\bar{1}$, is the twinning plane.
„ 13, Fig. 81. — Twinned octahedron. — Spinel, magnetite. — An octahedral face $11\bar{1}$, is the twinning-plane.
„ 14, Fig. 105. — Trapezohedron *n* (211). — Garnet, analcite, leucite.
„ 15, Fig. 106. — Dodecahedron *d* and trapezohedron *n* (211). — Garnet.
„ 16, Fig. 107. — Cube *a* and trapezohedron *n* (211). — Analcite.
„ 17, Fig. 108. — Dodecahedron *d* and trapezohedron *m* (311). — Magnetite. (Compare No. 15.)
„ 18, Fig. 109. — Trisoctahedron *p* (221). — Galena.
„ 19, Fig. 110. — Octahedron *o* and trisoctahedron *p* (221). — Galena.
„ 20, Fig. 111. — Tetrahexahedron *e* (210). — Copper.
„ 21, Fig. 112. — Cube *a* and tetrahexahedron *f* (310). — Fluorite.
„ 22, Fig. 113. — Hexoctahedron *s* (321).
„ 23, Fig. 114. — Dodecahedron *d* and hexoctahedron *s* (321). — Garnet.
„ 24, Fig. 115. — Cube *a* and hexoctahedron *t* (421). — Fluorite.

Pyritohedral Group of the Isometric System.

Models 25—33.

No. 25, Fig. 117. — Pyritohedron *e* (210). — Pyrite, cobaltite.
„ 26, Fig. 118. — Diploid *s* (321). — Pyrite.
„ 27, Fig. 120. — Cube *a* and pyritohedron *e* (210). — Pyrite. (Compare No. 7.)
„ 28, Fig. 121. — Octahedron *o* and pyritohedron *e* (210). — Pyrite.
„ 29, Fig. 122. — Octahedron *o* and pyritohedron *e* (210), both about equally developed. — Pyrite.
„ 30, Fig. 123. — Pyritohedron *e* (210) and octahedron *o*. — Pyrite.
„ 31, Fig. 124. — Cube *a*, pyritohedron *e* (210) and octahedron *ō*. — Pyrite.
„ 32, Fig. 125. — Diploid *t* (421) and cube *a*. — Pyrite.
„ 33, Fig. 126. — Pyritohedrons penetrating in twin position. — Pyrite. A dodecahedral face, 110, is the twinning-plane.

Tetrahedral Group of the Isometric System.

Models 34—44.

No. 34 and 35. — Tetrahedrons, which may be so orientated as to represent the positive form *o* (111), Fig. 128, and the negative form o_1 $(1\bar{1}1)$, Fig. 129. — Tetrahedrite, sphalerite, helvite.
„ 36, Fig. 130. — Tristetrahedron *n* (211). — Tetrahedrite.
„ 37, Fig. 131. — Deltoid dodecahedron (221).
„ 38, Fig. 132. — Hexakistetrahedron (321).
„ 39, Fig. 133. — Positive and negative tetrahedrons, *o* (111) and o_1 $(1\bar{1}1)$. — Sphalerite.
„ 40, Fig. 134. — Cube *a* and tetrahedron *o* (111). — Boracite. (Compare No. 4.)
„ 41, Fig. 135. — Tetrahedron *o* and cube *a*. — Boracite.
„ 42, Fig. 136. — Tetrahedron *o* and dodecahedron *d*. — Tetrahedrite.
„ 43, Fig. 137. — Dodecahedron *d*, cube *a*, and tetrahedron *o* (111). — Boracite. (Compare No. 10.)
„ 44, Fig. 138. — Tetrahedron *o* (111) and tristetrahedron *n* (211). — Tetrahedrite.

Tetragonal System.

Models 45—82.

Normal Group of the Tetragonal System.

Models 45—71.

No. 45, Fig. 142. — Pyramid of the first order *p* (111) of zircon; $c = 0.640$.
„ 46, Fig. 143. — Pyramid of the first order *p* (101) of braunite; $c = 0.895$. (Compare No. 2.)
„ 47, Fig. 144. — Pyramid of the first order *p* (111) of octahedrite; $c = 1.777$. The three foregoing forms all represent unit-pyramids (111), but, belonging to different minerals, they have different angles, hence different lengths of the vertical axis *c*.
„ 48, Fig. 145. — Pyramid of the second order *e* (101) of zircon; $c = 0.640$.
„ 49, Fig. 146. — Ditetragonal pyramid (311) of zircon; $c = 0.640$.
Models 50, 51 and 52 are constructed with equal axial lengths.
„ 50, Fig. 147. — Prism of the first order *m* (110), and base *c* (001).
„ 51, Fig. 148. — Prism of the second order *a* (100), and base *c* (001).
„ 52, Fig. 149. — Ditetragonal prism (210), and base *c* (001).
„ 53, Fig. 151. — Zircon: Prism *m* (110), and pyramid *p* (111).
„ 54, Fig. 152. — Zircon: Prism *m* (110), and pyramid *p* (111).
„ 55, Fig. 153. — Zircon: Prisms *m* (110) and *a* (100), and pyramid *p* (111).
„ 56, Fig. 154. — Zircon: Prism *m* (110), and pyramids, *u* (331) and *p* (111).
„ 57, Fig. 155. — Zircon: Prisms *m* (110) and *a* (100), ditetragonal pyramid *x* (311), and pyramid *p* (111).
„ 58, Fig. 156. — Vesuvianite: Prisms *m* (110) and *a* (100), and base *c* (001).
„ 59, Fig. 157. — Vesuvianite: Prisms *m* (110) and *a* (100), and pyramid *p* (111).
„ 60, Fig. 158. — Vesuvianite: Prism *m* (110), pyramid *p* (111), and base *c* (001).
„ 61, Fig. 159. — Vesuvianite: Prisms *m* (110) and *a* (100), pyramid *p* (111), and base *c* (001).
„ 62, Fig. 160. — Cassiterite: Pyramids *p* (111) and *e* (101).
„ 63, Fig. 161. — Cassiterite. Prisms *a* (100) and *m* (110), pyramids *e* (101) and *p* (111), and base *c* (001). The twinning-plane is *e* $(01\bar{1})$.
„ 64, Fig. 162. — Cassiterite: Prisms *m* (110) and *a* (100), and pyramids *p* (111) and *e* (101). The twinning-plane is *e* $(01\bar{1})$.
„ 65, Fig. 163. — Rutile: Prisms *m* (110) and *a* (100), and pyramids *p* (111) and *e* (101).
„ 66, Fig. 167. — Octahedrite: Pyramids *p* (111), *z* (113) and *x* (103).
„ 67, Fig. 168. — Octahedrite: Prism *a* (100), pyramid *p* (111), and base *c* (001).

No. 68, Fig. 169. — Apophyllite: Pyramid *p* (111), prism *a* (100), and base *c* (001).
„ 69, Fig. 170. — Apophyllite: Pyramid *p* (111) and prism *a* (100).
„ 70, Fig. 171. — Apophyllite: Pyramid *p* (111), prism *a* (100), ditetragonal prism *y* (310), and base *c* (001).
„ 71, Fig. 172. — Apophyllite: Pyramid *p* (111), prism *a* (100), and base *c* (001).

Tri-Pyramidal Group of the Tetragonal System.

Models 72—76.

No. 72, Fig. 173. — Scheelite: Pyramids of the second order *e* (101), of the first order *p* (111), and of the third order *s* (131).
„ 73, Fig. 175. — Scheelite: Pyramids *e* (101) and *p* (111).
„ 74, Fig. 176. — Scapolite: Prisms *m* (110) and *a* (100), and pyramid *p* (111).
„ 75, Fig. 177. — Scapolite: Prisms *m* (110) and *a* (100), and pyramid *p* (111).
„ 76, Fig. 178. — Scapolite: Prisms *m* (110) and *a* (100), and pyramids *p* (111) and *z* (311).

Sphenoidal Group of the Tetragonal System.

Models 77—82.

No. 77, Fig. 179. — Chalcopyrite: Sphenoid *p* (111). (Compare No. 34.)
„ 78, Fig. 180. — Chalcopyrite: Sphenoids *p* (111) and p_1 $(1\bar{1}1)$. (Compare No. 39.)
„ 79, Fig. 182. — Chalcopyrite: Shenoid *r* (332).
„ 80, Fig. 183. — Chalcopyrite: Pyramid of the second order *z* (201).
„ 81, Fig. 184. — Chalcopyrite: Pyramid *z* (201). The twinning-plane is $(\bar{1}\bar{1}1)$.
„ 82, Fig. 185. — Chalcopyrite: Sphenoid *Φ* (772) and scalenohedron *X* (122).

Hexagonal System.

Models 83—146.

Normal Group of the Hexagonal System.

Models 83—95.

Models 83 to 88 are constructed with equal axial lengths, that of the vertical axis being 1. 496, three times that of beryl.

No. 83, Fig. 191. — Pyramid of the first order $(10\bar{1}1)$; $c = 1.496$.
„ 84, Fig. 192. — Pyramid of the second order $(11\bar{2}2)$; $c = 1.496$.
„ 85, Fig. 193. — Ditetragonal pyramid $(21\bar{3}1)$ of beryl; $c = 0.499$.
„ 86, Fig. 194. — Prism of the first order *m* $(10\bar{1}0)$, terminated by the basal plane c (0001).
„ 87, Fig. 195. — Prism of the second order *a* $(11\bar{2}0)$, terminated by the basal plane c (0001).
„ 88, Fig. 197. — Dihexagonal prism $(21\bar{3}0)$, terminated by the basal plane c (0001).
„ 89, Fig. 199. — Beryl: Prism *m* $(10\bar{1}0)$, and pyramid *p* $(10\bar{1}1)$.
„ 90, Fig. 200. — Beryl: Prism *m* $(10\bar{1}0)$, base *c* (0001), and pyramid of the second order *s* $(11\bar{2}1)$.
„ 91, Fig. 201. — Beryl: Prism *m* $(10\bar{1}0)$ and pyramid *p* (1011) of the first order, prism *a* $(11\bar{2}0)$ and pyramid *s* $(11\bar{2}1)$ of the second order, and base *c* (0001).
„ 92, Fig. 203. — Beryl: Prism *m* $(10\bar{1}0)$ and pyramid *p* (1011) of the first order, pyramids *s* $(11\bar{2}1)$ and *d* $(33\bar{6}4)$ of the second order, dihexagonal pyramid *n* $(31\bar{4}1)$, and base *c* (0001).
„ 93, Fig. 204. — Pyrrhotite: Prism *m* $(10\bar{1}0)$, and base *c* (0001).

No. 94, Fig. 205. — Pyrrhotite: Prism *m* $(10\bar{1}0)$, pyramids of the first order, *p* $(10\bar{1}1)$ and *u* $(40\bar{4}1)$, and base *c* (0001).
„ 95, Fig. 206. — Hanksite: Prism *m* $(10\bar{1}0)$ and pyramid *p* $(10\bar{1}1)$ of the first order, and base *c* (0001).

Tri-Pyramidal Group of the Hexagonal System.

Models 96—99.

No. 96, Fig. 207. — Apatite: Prism *m* $(10\bar{1}0)$ and three pyramids of the first order, *r* $(10\bar{1}2)$, *p* $(10\bar{1}1)$ and *y* $(20\bar{2}1)$, prism *a* $(11\bar{2}0)$ and pyramid *s* $(11\bar{2}1)$ of the second order, pyramid of the third order *u* $(21\bar{3}1)$, and base *c* (0001).
„ 97, Fig. 209. — Apatite: Prism *m* $(10\bar{1}0)$ and pyramid *p* $(10\bar{1}1)$.
„ 98, Fig. 210. — Apatite: Prism *m* $(10\bar{1}0)$, pyramid *p* $(10\bar{1}1)$, and base *c* (0001).
„ 99, Fig. 211. — Vanadinite: Prism *m* $(10\bar{1}0)$, base *c* (0001), and pyramid of the third order *u* $(21\bar{3}1)$.

Hemimorphic Group of the Hexagonal System.

Models 100—101.

No. 100, Fig. 212. — Jodyrite: Prism of the second order *a* $(11\bar{2}0)$, terminated above by an acute pyramid of the first order *u* $(40\bar{4}1)$ and the base *c* (0001), and below by an obtuse pyramid *π* $(40\bar{4}5)$.
„ 101, Fig. 213. — Zincite: Prism of the first order m $(10\bar{1}0)$, terminated above by the pyramid *p* $(10\bar{1}1)$, and below by the base c (0001).

Rhombohedral Groups of the Hexagonal System.

Models 102—146.

Normal Rhombohedral Group of the Hexagonal System.

Models 102—127.

No. 102 and 103. — Rhombohedrons, which may be so orientated as to represent the positive form *r* $(10\bar{1}1)$, Fig. 215, and the negative form $(01\bar{1}1)$, Fig. 216; $c = 0.854$.
„ 104, Fig. 217. — Scalenohedron $(21\bar{3}1)$; $c = 0.854$.
„ 105, Fig. 218. — Calcite: Negative rhombohedron *e* $(01\bar{1}2)$.
„ 106, Fig. 220. — Calcite: Negative rhombohedron *h* $(03\bar{3}2)$.
„ 107, Fig. 221. — Calcite: Negative rhombohedron *f* $(02\bar{2}1)$.
„ 108, Fig. 222. — Calcite: Negative rhombohedron *f* $(02\bar{2}1)$ and positive rhombohedron *r* $(10\bar{1}1)$.
„ 109, Fig. 223. — Calcite: Positive rhombohedron *M* $(40\bar{4}1)$ and base *c* (0001).
„ 110, Fig. 224. — Calcite: Positive rhombohedron *p* $(16.\ 0.\ \overline{16}.\ 1)$ and base *c* (0001). (Compare No. 111.)
„ 111, Fig. 225. — Calcite: Prism *m* $(10\bar{1}0)$ and base *c* (0001).
„ 112, Fig. 226. — Calcite: Prism *m* $(10\bar{1}0)$ and negative rhombohedron *e* $(01\bar{1}2)$.
„ 113, Fig. 227. — Calcite: Prism *m* $(10\bar{1}0)$ and negative rhombohedron *e* $(01\bar{1}2)$. The twinning-plane is *r* $(01\bar{1}\bar{1})$. Since $c \wedge r = 44^0\ 36^1/_3{}'$, the vertical axes in twin position are nearly at right angles to each other.
„ 114, Fig. 228. — Calcite: Prism *m* $(10\bar{1}0)$, negative rhombohedron *e* $(01\bar{1}2)$, and base *c* (0001).
„ 115, Fig. 230. — Calcite: Scalenohedron *v* $(21\bar{3}1)$. The twinning-plane is *c* (0001).

No. 116, Fig. 231. — Calcite: Scalenohedron v $(21\bar{3}1)$, and rhombohedron r $(10\bar{1}1)$.
„ 117, Fig. 232. — Calcite: Prism m $(10\bar{1}0)$ and scalenohedron v $(21\bar{3}1)$.
„ 118, Fig. 233. — Calcite: Prism m (1010), scalenohedron v $(21\bar{3}1)$, and negative rhombohedron e $(01\bar{1}2)$.
„ 119, Fig. 234. — Corundum: Prism of the second order a $(11\bar{2}0)$, rhombohedron r $(10\bar{1}1)$, and base c (0001).
„ 120, Fig. 235. — Corundum: Prism a $(11\bar{2}0)$, pyramid n $(22\bar{4}3)$, rhombohedron r $(10\bar{1}1)$, and base c (0001)
„ 121, Fig. 236. — Corundum: Prism a $(11\bar{2}0)$, pyramid n $(22\bar{4}3)$, rhombohedron r $(10\bar{1}1)$, and base c (0001).
„ 122, Fig. 237. — Hematite: Rhombohedron r $(10\bar{1}1)$.
„ 123, Fig. 238. — Hematite: Rhombohedron r $(10\bar{1}1)$, and base c (0001).
„ 124, Fig. 239. — Hematite: Rhombohedrons r $(10\bar{1}1)$ and u $(10\bar{1}4)$, and pyramid of the second order n $(22\bar{4}3)$.
„ 125, Fig. 240. — Hematite: Rhombohedron r $(10\bar{1}1)$, negative rhombohedron s $(02\bar{2}1)$, pyramid of the second order n $(22\bar{4}3)$, and base c (0001).
„ 126, Fig. 241. — Hematite: Very flat negative rhombohedron x $(0.\ 1.\ \bar{1}.\ 12)$, and base c (0001).
„ 127, Fig. 242. — Chabazite: Rhombohedron r $(10\bar{1}1)$, with two negative rhombohedrons, e $(01\bar{1}2)$ and f $(02\bar{2}1)$.

Hemimorphic-Rhombohedral Group of the Hexagonal System.

Models 128—131.

No. 128, Fig. 244. — Tourmaline: Prisms of the first order m $(10\bar{1}0)$ and of the second order a $(11\bar{2}0)$, terminated by rhombohedral-like forms r $(10\bar{1}1)$ above, and r $(01\bar{1}\bar{1})$ below.
„ 129, Fig. 245. — Tourmaline: Prisms of the first order m (1010) and of the second order a $(11\bar{2}0)$, terminated by rhombohedral-like forms r $(10\bar{1}1)$ and o $(02\bar{2}1)$ above, and r $(01\bar{1}\bar{1})$ below.
„ 130, Fig. 246. — Tourmaline: Prisms of the first order m $(10\bar{1}0)$ and of the second order a $(11\bar{2}0)$, terminated above by the rhombohedral-like form o $(02\bar{2}1)$, and below by the rhombohedral-like form r $(01\bar{1}\bar{1})$, and the base c $(000\bar{1})$.
„ 131, Fig. 247. — Tourmaline: Prisms of the first order m $(10\bar{1}0)$ and of the second order a $(11\bar{2}0)$, terminated above by the scalenohedral-like form u $(32\bar{5}1)$ and the rhombohedral-like form o $(02\bar{2}1)$, and below by two rhombohedral-like forms r $(01\bar{1}\bar{1})$ and o $(20\bar{2}\bar{1})$.

Tri-Rhombohedral Group of the Hexagonal System.

Models 132—136.

No. 132, Fig. 248. — Phenacite: Prism of the second order a $(11\bar{2}0)$ and rhombohedron of the third order x $(21\bar{3}2)$.
„ 133, Fig. 249. — Willemite: Prism of the second order a $(11\bar{2}0)$, rhombohedrons of the first order r (1011) and e $(01\bar{1}2)$, rhombohedron of the second order u $(2\bar{1}\bar{1}3)$, and base c (0001).
„ 134, Fig. 250. — Dioptase: Prism of the second order a (1120) and rhombohedron of the first order s $(02\bar{2}1)$.
„ 135, Fig. 251. — Dioptase: Prism of the second order a $(11\bar{2}0)$, rhombohedron of the first order s $(02\bar{2}1)$, and rhombohedron of the third order x $(13\bar{4}1)$.
„ 136, Fig. 252. — Ilmenite: Rhombohedrons of the first order r $(10\bar{1}1)$ and of the second order n $(22\bar{4}3)$, and base c (0001).

Trapezohedral Group of the Hexagonal System.

Models 137—146.

No. 137, Fig. 253. — Quartz: Prism of the first order m $(10\bar{1}0)$, and rhombohedrons r $(10\bar{1}1)$ and z $(01\bar{1}1)$.
„ 138, Fig. 254. — Quartz: Rhombohedrons r $(10\bar{1}1)$ and z $(01\bar{1}1)$.
„ 139, Fig. 255. — Quartz: Prism m $(10\bar{1}0)$, and rhombohedrons r $(10\bar{1}1)$ and z $(01\bar{1}1)$.
„ 140, Fig. 256. — Quartz: Prism m $(10\bar{1}0)$. rhombohedrons r $(10\bar{1}1)$, z $(01\bar{1}1)$, trigonal pyramid s $(11\bar{2}1)$, and trapezohedron x $(51\bar{6}1)$. The model represents a right-handed crystal.
„ 141, Fig. 257. — Quartz: Prism m $(10\bar{1}0)$, rhombohedrons r $(10\bar{1}1)$ and z $(01\bar{1}1)$, trigonal pyramid s $(2\bar{1}\bar{1}1)$, and trapezohedron x $(61\bar{5}1)$. The model represents a left-handed crystal.
„ 142 and 143, Figs. 258 and 259. — Right and left-handed trapezohedrons $(21\bar{3}1)$ and $(\bar{2}3\bar{1}1)$.
„ 144, Fig. 260. — Trigonal pyramid of the second order $(11\bar{2}1)$.
„ 145, Fig. 261. — Quartz: Prism m (1010), positive rhombohedrons r $(10\bar{1}1)$ and M $(30\bar{3}1)$, negative rhombohedrons z $(01\bar{1}1)$ and M_1 $(03\bar{3}1)$, and trigonal pyramid s $(2\bar{1}\bar{1}1)$.
„ 146, Fig. 262. — Quartz: Prism m $(10\bar{1}0)$, positive rhombohedrons r $(10\bar{1}1)$ and M $(30\bar{3}1)$, and negative rhombohedrons z $(01\bar{1}1)$ and M_1 $(03\bar{3}1)$.

Orthorhombic System.

Models 147—185.

Normal Group of the Orthorhombic System.

Models 147—183.

Models 147 to 151 are constructed with equal axial lengths.

No. 147, Fig. 268. — Pyramid p (111).
„ 148, Fig. 269. — Prism m (110), and base c (001).
„ 149, Fig. 270. — Macro-dome (101), and brachy-pinacoid b (010).
„ 150, Fig. 271. — Brachy-dome (011), and marco-pinacoid a (100).
„ 151, Fig. 272. — Macro-pinacoid a (100), brachy-pinacoid b (010), and base c (001).
„ 152, Fig. 273. — Barite: Prism m (110) and base c (001).
„ 153, Fig. 274. — Barite: Prism m (110), base c (001), macro-dome d (102), and brachy-dome o (011).
„ 154, Fig. 275. — Barite: Prism m (110), base c (001), and macro-dome d (102).
„ 155 and 156, Figs. 276 and 277. — Barite: Macro-dome d (102), brachy-dome o (011), and base c (001).
„ 157, Fig. 278. — Celestite: Prism m (110), two macro-domes d (102) and l (104), brachy-dome o (011), and base c (001).
„ 158, Fig. 279. — Celestite: Prism m (110), macro-dome d (102), brachy-dome o (011), and base c (001).
„ 159, Fig. 281. — Sulphur: Pyramids p (111) and s (113).
„ 160, Fig. 282. — Sulphur: Pyramids p (111) and s (113), brachy-dome n (011) and base c (001).
„ 161, Fig. 283. — Stibnite: Prism m (110), brachy-pinacoid b (010), and pyramid s (113).
„ 162, Fig. 284. — Stibnite: Prism m (110), brachy-pinacoid b (010), and pyramids p (111) and r (343).
„ 163, Fig. 285. — Arsenopyrite: Prism m (110) and brachy-dome u (014).
„ 164, Fig. 286. — Arsenopyrite: Prism m (110) and brachy-dome q (011).

No. 165, Fig. 287. — Chalcocite: Prism *m* (110), pyramid *v* (112), brachy-pinacoid *b* (010), brachy-dome *d* (021), rounded brachy-domes, and base *c* (001).

„ 166, Fig. 288. — Chalcocite: Prism *m* (110), pyramids *p* (111) and *v* (112), brachy-pinacoid *b* (010) and brachy-dome *d* (021).

„ 167, Fig. 289. — Topaz: Prisms *m* (110) and *l* (120), and pyramid *p* (111).

„ 168, Fig. 290. — Topaz: Prisms *m* (110) and *l* (120), pyramid *o* (221), brachy-dome *f* (021) and macro-dome *d* (201).

„ 169, Fig. 291. — Topaz: Prisms *m* (110) and *l* (120), pyramids *p* (111) and *i* (223), brachy-dome y (041) and base *c* (001).

„ 170, Fig. 292. — Topaz: Prisms *m* (110) and *l* (120), brachy-pinacoid *b* (010), pyramid *o* (221), brachy-dome *y* (041) and base *c* (001).

„ 171, Fig. 293. — Topaz: Prisms *m* (110) and *l* (120), brachy-pinacoid *b* (010), pyramids *o* (221) and *p* (111), brachy-domes *f* (021) and *y* (041), macro-dome *d* (201) and base *c* (001).

„ 172, Fig. 294. — Chrysolite: Macro-pinacoid *a* (100), brachy-pinacoid *b* (010), prism *m* (110), pyramid *p* (111), macro-dome *d* (101), brachy-dome *k* (021), and base *c* (001).

„ 173, Fig. 295. — Chrysolite: Prisms *m* (110) and *s* (120), brachy-pinacoid *b* (010), brachy-dome *k* (021), macro-dome *d* (101) and pyramid *p* (111).

„ 174, Fig. 297. — Staurolite: Prism *m* (110), brachy-pinacoid *b* (010), and base *c* (001).

„ 175, Fig. 298. — Staurolite: Prism *m* (110), brachy-pinacoid *b* (010), macro-dome *r* (101), and base *c* (001).

„ 176, Fig. 299. — Staurolite: Prism *m* (110), brachy-pinacoid *b* (010), macro-dome *r* (101) and base *c* (001). A brachy-dome (032) is the twinning-plane.

„ 177, Fig. 300. — Staurolite: Prism *m* (110), brachy-pinacoid *b* (010), and base *c* (001). A pyramid ($\bar{2}$32) is the twinning plane.

„ 178, Fig. 301. — Aragonite: Prism *m* (110), brachy-pinacoid *b* (010), pyramid *i* (661) and brachy-domes *j* (0. 12. 1) and *k* (011).

„ 179, Fig. 302. — Aragonite: Prism *m* (110), brachy-pinacoid *b* (010), and brachy-dome *k* (011).

„ 180 and 181, Figs. 303 and 304. — Aragonite: Prism *m* (110), brachy-pinacoid *b* (010), and brachy-dome *k* (011). The twinning-plane is *m* (1$\bar{1}$0).

„ 182, Fig. 308. — Cerussite: Prism *m* (110), brachy-pinacoid *b* (010) and pyramid *p* (111). Penetration of three crystals in twin position, the twinning-plane being *m* (1$\bar{1}$0).

„ 183, Fig. 309. — Childrenite: Macro-pinacoid *a* (100), brachy-pinacoid *b* (010), and pyramid *s* (121).

Hemimorphic Group of the Orthorhombic System.

No. 184, Fig. 310. — Calamine: Prism *m* (110), macro-pinacoid *a* (100), and brachy-pinacoid *b* (010), terminated above by the macro-dome *t* (301), brachy-dome *i* (031) and base *c* (001), and terminated below by the pyramid *v* (12$\bar{1}$).

Sphenoidal Group of the Orthorhombic System.

No. 185, Fig. 311. — Epsomite: Prism *m* (110) and sphenoid *z* (111).

Monoclinic System.

Models 186—212.

Normal Group of the Monoclinic System.

Models 186 to 190 are constructed with the same axial lengths.

No. 186, Fig. 317. — Pyramid, consisting of two independent forms, each having four faces, *p* (111) and *o* ($\bar{1}$11). As to the significance of the name **pyramid** as applied to the monoclinic system, see page 209 of the text.

No. 187, Fig. 318. — Prism *m* (110) and base *c* (001).

„ 188, Fig. 319. — Clino-dome (011) and ortho-pinacoid *a* (100).

„ 189, Fig. 320. — Two ortho-domes (101) and ($\bar{1}$01), and clino-pinacoid *b* (010).

„ 190, Fig. 321. — Ortho-pinacoid *a* (100), clino-pinacoid *b* (010) and base *c* (001).

„ 191, Fig. 322. — Gypsum: Prism *m* (110), clino-pinacoid *b* (010), and pyramid *p* (11$\bar{1}$).

„ 192, Fig. 323. — Gypsum: Prism *m* (110), clino-pinacoid *b* (010), and pyramid *p* (11$\bar{1}$).

„ 193, Fig. 324. — Gypsum: Prism *m* (110), clino-pinacoid *b* (010), pyramid *p* (111), and ortho-dome *e* ($\bar{1}$03).

„ 194, Fig. 325. — Gypsum: Prism *m* (110), clino-pinacoid *b* (010), and pyramid *p* (11$\bar{1}$). The twinning-plane is the ortho-pinacoid *a* (100).

„ 195, Fig. 326. — Orthoclase: Prism *m* (110), clino-pinacoid *b* (010), ortho-dome *y* (20$\bar{1}$) and base *c* (001).

„ 196, Fig. 327. — Orthoclase: Prism *m* (110), clino-pinacoid *b* (010), ortho-domes *x* (10$\bar{1}$) and *y* (20$\bar{1}$) and base *c* (001).

„ 197, Fig. 328. — Orthoclase: Prisms *m* (110) and *z* (130), orthodomes *x* (10$\bar{1}$) and *y* (20$\bar{1}$), pyramid *o* (11$\bar{1}$), and base *c* (001).

„ 198, Fig. 329. — Orthoclase: Prism *m* (110), clino-pinacoid *b* (010), ortho-dome *y* (20$\bar{1}$) and base *c* (001). So-called Carlsbad twin, the vertical axis is the twinning-axis, the clino-pinacoid *b* is the composition face.

„ 199, Fig. 330. — Pyroxene: Ortho-pinacoid *a* (100), clino-pinacoid *b* (010), base *c* (001), prism *m* (110), and pyramid *p* (111).

„ 200, Fig. 331. — Pyroxene: Ortho-pinacoid *a* (100), clino-pinacoid *b* (010), base *c* (001), ortho-dome *d* (10$\bar{1}$), and pyramids *p* (111) and *v* (221).

„ 201, Fig. 332. — Pyroxene: Ortho-pinacoid *a* (100), clino-pinacoid *b* (010), prism *m* (110) and two pyramids *p* (111) and *o* (22$\bar{1}$).

„ 202, Fig. 333. — Pyroxene: Ortho-pinacoid *a* (100), clino-pinacoid *b* (010), base *c* (001), prism *m* (110), ortho-dome *d* (10$\bar{1}$), and pyramids *p* (111) and *s* (11$\bar{1}$).

„ 203, Fig. 335. — Pyroxene, variety augite: Ortho-pinacoid *a* (100), clino-pinacoid *b* (010), prism *m* (110) and pyramid *s* (11$\bar{1}$).

„ 204, Fig. 336. — Pyroxene, variety augite: Ortho-pinacoid *a* (100), clino-pinacoid *b* (010), prism *m* (110), pyramid *s* (11$\bar{1}$) and ortho-dome *n* ($\bar{1}$02).

„ 205, Fig. 337. — Amphibole: Prism *m* (110) and clino-dome *r* (011).

„ 206, Fig. 338. — Amphibole: Prism *m* (110), clino-pinacoid *b* (010) and clino-dome *r* (011).

„ 207, Fig. 339. — Amphibole: Ortho-pinacoid *a* (100), clino-pinacoid *b* (010), two prisms *m* (110) and *e* (130), and clino-dome *r* (011).

„ 208, Fig. 340. — Titanite: Prism *m* (110), pyramid *p* (111), and base *c* (001).

„ 209, Fig. 341. — Titanite: Ortho-pinacoid *a* (100), base *c* (001), prism *m* (110), and pyramid *p* (111).

„ 210, Fig. 342. — Titanite: Prism *m* (110) and pyramid *p* (111).

„ 211, Fig. 343. — Epidote: Ortho-pinacoid *a* (100), base *c* (001), ortho-dome *r* (10$\bar{1}$), and pyramid *n* (11$\bar{1}$).

„ 212, Fig. 344. — Epidote: Ortho-pinacoid *a* (100), clino-pinacoid *b* (010), base *c* (001), ortho-domes *r* (10$\bar{1}$) and *i* ($\bar{1}$02), clino-domes *o* (011) and *k* (012), prism *m* (110), and pyramids *p* (111) and *n* (11$\bar{1}$).

Triclinic System.

Models 213—225.

Normal Group of the Triclinic System.

Models 213 to 217 are constructed with the same axial lengths.

No. 213, Fig. 347. — Pyramid, consisting of four independent forms, each having two faces, (111), $(1\bar{1}1)$, $(11\bar{1})$ and $(1\bar{1}\bar{1})$. As to the significance of the names pyramid, prism and dome, as applied to the triclinic system, see page 215 of the text.

„ 214, Fig. 348. — Prisms *m* (110) and *M* $(1\bar{1}0)$, and base *c* (001).

„ 215, Fig. 349. — Macro-domes (101) and $(10\bar{1})$, and brachy-pinacoid *b* (010).

„ 216, Fig. 350. — Brachy-domes (011) and $(01\bar{1})$, and macro-pinacoid *a* (100).

„ 217, Fig. 351. — Macro-pinacoid *a* (100), brachy-pinacoid *b* (010) and base *c* (001).

„ 218, Fig. 352. — Axinite: Macro-pinacoid *a* (100), prisms *m* (110) and *M* $(1\bar{1}0)$, macro-dome *s* (201) and pyramids *p* (111) and *r* $(1\bar{1}1)$.

„ 219, Fig. 353. — Albite: Brachy-pinacoid *b* (010), base c (001), prisms *m* (110) and *M* $(1\bar{1}0)$, and pyramids *o* $(11\bar{1})$ and *q* $(1\bar{1}\bar{1})$.

„ 220, Fig. 354. — Albite, pericline type: Brachy-pinacoid *b* (010), base *c* (001), prisms *m* (110) and *M* $(1\bar{1}0)$, macro-dome *x* $(10\bar{1})$ and pyramid *o* $(11\bar{1})$.

„ 221, Fig. 355. — Albite: Brachy-pinacoid *b* (010), base *c* (001), prisms *m* (110) and *M* $(1\bar{1}0)$, macro-dome *x* $(10\bar{1})$ and pyramid *o* $(11\bar{1})$. The brachy-pinacoid *b* is the twinning-plane: Albite law.

„ 222, Fig. 356. — Albite: Brachy-pinacoid *b* (010), base c (001), prisms *m* (110) and *M* $(1\bar{1}0)$, and macro-dome *x* $(10\bar{1})$. Polysynthetic twin: Albite law.

„ 223, Fig. 357. — Cyanite: Macro-pinacoid *a* (100), brachy-pinacoid *b* (010), base c (001) and prism *M* $(1\bar{1}0)$.

„ 224, Fig. 358. — Rhodonite: Macro-pinacoid *a* (100), base *c* (001), prisms *m* (110) and *M* $(1\bar{1}0)$, and pyramids *n* $(22\bar{1})$ and *k* $(2\bar{2}\bar{1})$.

„ 225, Fig. 359. — Chalcanthite: Macro-pinacoid *a* (100), brachy-pinacoid *b* (010), prisms *m* (110) and *M* $(1\bar{1}0)$ and pyramid *p* (111).

THE PENFIELD CONTACT GONIOMETER.

Designed and Patented by S. L. PENFIELD,

Professor in Yale University, New Haven, Conn.

Model A.

This instrument consists of two parts; a pair of measuring arms or straight-edges, which may be set at any angle and thus be made to correspond with any desired angle of a crystal, figure 1, and a graduated card for measuring the angular divergence of the arms. Two pairs of measuring arms are supplied with each instrument; a pair made of strips of hard fiber, and a pair made of a strip of hard fiber and a strip of transparent celluloid. The celluloid strip is blackened for a portion of its length, figure 1, and a fine line is scratched on its under surface

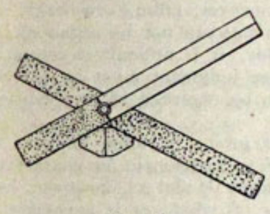

Fig. 1.

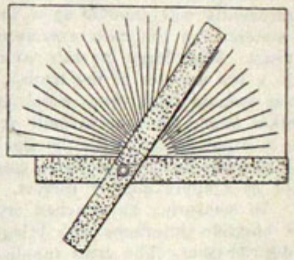

Fig 2.

exactly parallel with its edges. The card, figure 2, has a graduation of a special design printed on it, each degree being represented by a long line continued to near the center. After having applied the arms to a crystal, the are brought in contact with the card as shown in figure 2; the upper one resting on the surface of the card, the lower one held firmly against the base-line. The arms are then moved until their point of divergence is at the center, when an edge of the upper arm will be parallel, or nearly so, to some line of the graduation which indicates the degree. In case the arms having one strip of celluloid, figure 1, are employed, the celluloid arm is made to rest on the surface of the card, and the angle is most conveniently determined by bringing the fine line scratched on its under surface to the center and noting its position with reference to the long degree lines on the card.

Prices:

1 Goniometer, Model A	=	*M* 2.50
10 „ „ „	=	„ 21.25 ($ 5.—)

Model B.

This instrument, figure 3, consists of a graduated semicircle printed on a card, in combination with an arm of transparent celluloid, swiveled by means of an eyelet at the center of the semicircle. A fine index-line scratched on the under side of the celluloid arm, parallel to its edges and exactly in line with the center of the eyelet, serves to indicate the angle which the arm makes with the base-line of the card. As it is at times difficult to bring a transparent edge exactly in contact with a crystal face, the celluloid arm for a portion of its length and the lower edge of the card have been blackened.

In using the instrument for measuring the interfacial angles of a crystal, the card is held at rigth angles to the edge formed by the meeting of two faces, and the arm is adjusted so that its edge and the base-line of the card, figure 3, come as nearly as possible in contact with the two faces.

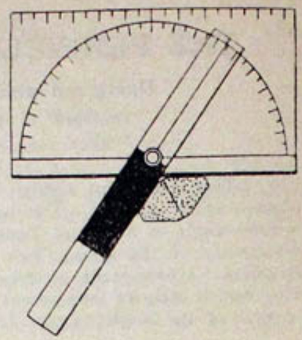

Fig. 3.

In measuring the angles of a crystal it is generally best to hold the crystal about on a level with the eye, and adjust the arms in contact with its faces when looking toward a strong light. The adjustment is as exact as possible when the opaque edges of the arms come in such close contact with the crystal faces as to cut off all the light, or, the crystal faces being somewhat uneven, as to leave only a little light showing. The accuracy of the measurements will depend upon the character of the material an the care exercised in adjusting the arms. With large crystals having smooth faces, measurements ought to be made within a few minutes of the truth. Large crystals, however, often have rough, uneven, or striated faces, from which accurate measurements can not be obtained. On the other hand, when only small crystals are available, it is difficult to adjust the arms in exact contact with the small surfaces. Hence judgment must be exercised in all cases in deciding whether measurements are to be regarded as very trustworthy or only approximately correct.

In measuring an attached crystal, or one of a group, it often happens that some obstacle interferes with bringing the arms of an instrument in contact with the desired faces. The arms supplied with the instrument (Model A), however, being inexpensive, their ends may be shortened by cutting off whatever is necessary, so that when applied they are clear of the obstruction.

There may be many uses for this instrument in offices of architects, designers, stonecutters, pattern makers, and engineers. Figures 4 and 5, for example, illustrate how the arms may be shortened in order that the angle in a notch or an internal angle may be measured.

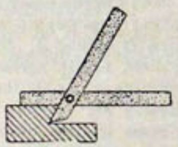

Fig. 4.

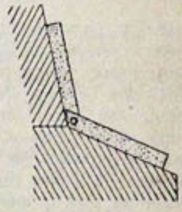

Fig. 5.

In describing the forms of crystals, two kinds of angles may be employed; the real and the supplement. As illustrated by figure 6, which represents the cross-section of an amphibole crystal, its faces m and m''' meet at an angle of 124° 11'. There are, however, many advantages to be gained by using the supplement angle 55° 49', as will be shown.

Let it be imagined that the crystal is within a circle, figure 7, and that normals n are drawn from the center of the circle at right angles to the crystal faces, until they meet the circumference; the angles between the normals, which may be measured on the circumference, correspond to the supplement angles of the crystal faces. Advantages derived from the use of supplement angles, or the angles between normals, are as follows:

Measuring completely around a crystal, in a zone, from one face to another, the angles add up to 360°. The angle between the prism m and the truncating face a, figures 6 and 7, is 27° $54^1/_2$, one half of $m \wedge m'''$ (55° 49'). Likewise the angle between the prism m and the truncating face b, at the side, is 62° $5^1/_2$', the complement of $m \wedge a$ (27° $54^1/_2$'), also one half of $m \wedge m'$ (124° 11'). Thus, having a record of a single supplement angle, such as $m \wedge m'''$, numerous other angles may be derived from the one value by a simple mental calculation.

Supplement angles are the ones obtained directly from the readings of the circle when a reflection goniometer is used. For purposes of calculation, as in the mathematical treatment of crystallography, supplement angles are far easier and

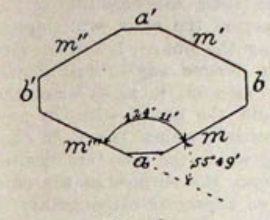

Fig. 6.

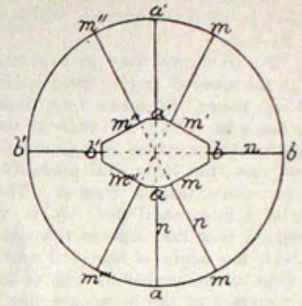

Fig. 7.

more convenient to use than real ones; hence they are universally employed by crystallographers.

Learning to use supplement angles presents almost no difficulty, even to a beginner; hence any one having a goniometer can well afford to learn the best and only true scientific method.

Prices:

1	Goniometer, Model B	= *M* 2.50
10	„ „ „	= „ 21 25 ($ 5.—)

THE PENFIELD ARM PROTRACTOR AND GONIOMETER.

Designed and Patented by S. L. PENFIELD,

Professor in Yale University, New Haven, Conn.

This instrument consists of a graduated semicircle printed on a card, in combination with an arm of transparent celluloid, swiveled by means of an eyelet at the center of the semicircle. A fine index-line, scratched on the under side of the celluloid arm parallel to its edges, indicates by its position with reference to the graduation the angle which the arm makes with the base-line of the card. The graduated semicircle is printed with its 0°—180° line exactly parallel with the upper and lower edges of the card, and the eyelet is so placed that its center is in alinement both with the 0°—180° line of the graduation and the index-line of the celluloid arm. A test of the accuracy of the adjustment may be made by noting that the index-line of the arm coincides with the 0°—180° line of the semicircle in two positions; when the longer end of the arm is either to the left, or, after turning 180°, to the right, of the center.

The materials of which the instrument are made have been very carefully considered. The card is of the best quality, very firm and strong, and capable of withstanding a great deal of wear. The celluloid strips are prepared with much care, the edges being straight, smooth, and parallel. The eyelet, before being turned or clinched, is swelled so that it just fits the holes punched in the card and celluloid, thus avoiding any lateral motion. It has a smooth and comparatively large wearing surface, and, the motion of the arm being always slow, the instrument may be used for a long time without showing appreciable wear at the joint. If in time the joint should become loose it may be tightened by gentle hammering of the eyelet.

In addition to being inexpensive, convenient, and very accurate, the instrument has certain other advantages which are set forth in the following statements explaining its uses:

To draw two lines at a given angle it is simply necessary to set the index-line at the desired angle, and, holding the card and the celluloid arm firmly on a sheet of paper, to make two lines with a pencil, one along the base-line of the card, the other along the edge of the arm. The accuracy of the work will depend upon the care exercised in adjusting the arm and drawing the lines. If drawn with proper care the lines will probably be within 3′ of the desired angle, and should not vary more than 5′ from it. The eror should not amount to more than the width of a fine pencil line. It is very important to hold the pencil with its axis so inclined that that side of the pencil lead shall be vertical which comes in contact with the edges of the card and celluloid arm along which the lines are drawn. The drop of the projecting end of the celluloid arm, from the surface of the card to the surface of the drawing-paper, is so slight that no appreciable inaccuracy is caused thereby. If the drop is objectionable, a strip of cardboard may be placed under the celluloid, or a small piece of card or blotting-paper may be fastened permanently with glue to that end of the celluloid arm which projects beyond the card.

It will be observed that the instrument does not need to be adjusted to a base-line and centered at some specific point, as is the case with most protractors. The lines are drawn not to the center of the eyelet, but parallel, respectively, to the 0°—180° line of the semicircle and the index-line of the celluloid arm.

When used in connection with a T-square, the protractor is admirably adapted for laying off angles quickly and accurately. With the arm set at 30°, 45°, 60°, 90°, or any other desired angle, it may be used as a drafting instrument in place of the ordinary triangles. By placing a mark on the T-square and making use of the divisions of the scale on the edge of the card, very evenly spaced section lines may be drawn.

The scales printed on the card are the ones generally needed. The decimal one on the upper edge may be used in connection with angles for plotting all kinds of problems in geometry and trigonometry. If figures are carefully drawn to scale, most problems may be solved graphically, wich is a very important consideration, since a graphical solution may be in itself sufficient for a demonstration, or it may be used as a check on the results to a numerical calculation.

The square with horizontal and diagonal lines, within the semicircle, measures just an inch on a side, and by means of it any desired hundredths of an inch may be determined. For example, to lay of $^{67}/_{100}$ of an inch: On the upper horizontal line go to the sixth space ($^{6}/_{10}$ of an inch), then down the diagonal to the seventh horizontal line. From the point thus found to the right hand vertical line is $^{67}/_{100}$ of an inch ($^{6}/_{10} + ^{7}/_{100}$). The scales and also the graduation of the semicircle are engine-divided, which is equivalent to a guarantee of their accuracy.

In addition to being a protractor, the instrument is also an accurate *goniometer*. For measuring plane angles, adjust the arm so that when the instrument is applied to a drawing, the base-line of the card and an edge of the arm are parallel, respectively, to two lines of the drawing or figure. In measuring an angle made by two plane surfaces, hold the card at right angles to the edge formed by the surfaces, and then adjust the arm so that when the base-line of the card is in contact with one surface, an edge of the arm is in contact with the other. If the surfaces are large and plane, very accurate measurements may be thus made.

Prices:

1 Arm Protractor	. . . . =	*M* 2.50
10 " "	. . . . =	" 21.25 ($ 5.—)

New Geotectonic Models

for the illustration of the

Architecture of the Earth's Crust

Construeted by Prof. Dr. L. Duparc (Geneva)
and by Prof. Dr. A. Schmidt (Bale).

These models, made of plaster, are constructed in such a manner as to show not only the geological features of the surface, but also on the sides diagram-sections illustrate the structure of the underlying crust. To each such model belongs a cap representing the masses of rocks, which are supposed to have been worn away by denudation and showing the way in which the folding of the Strata has taken place. The motives are taken from some of the most interesting parts of the Alps and the Jura Mt. in Switzerland, among those also two different representations of the renowned **„Glärner double fold with inversion and thrust-plane“.**

Prize of the set of 8 models by Prof Dr. L. Duparc
size about ca. 40×20×10 cm, the Glärner double fold about
100×22×10 cm . . . . *M* 360.—

Prize of the Glärner-double-fold-model by Prof. Dr. A. Schmidt
size about ca. 100×22×10 cm . . . . *M* 100.—

(An accurate description of these models will be sent free
on application)
conf. Catalogue No. 2a: Geology.
(2d ed. 1901)

Bonn, Printed by Charles Georgi.